

Article

## The Stereochemical Consequences of Vinylpyruvate Hydratase-catalyzed Reactions

William H. Johnson, Tyler M.M. Stack, Stephanie M Taylor, Elizabeth A Burks, and Christian P. Whitman

*Biochemistry*, **Just Accepted Manuscript** • DOI: 10.1021/acs.biochem.6b00552 • Publication Date (Web): 30 Jun 2016

Downloaded from <http://pubs.acs.org> on July 9, 2016

### Just Accepted

"Just Accepted" manuscripts have been peer-reviewed and accepted for publication. They are posted online prior to technical editing, formatting for publication and author proofing. The American Chemical Society provides "Just Accepted" as a free service to the research community to expedite the dissemination of scientific material as soon as possible after acceptance. "Just Accepted" manuscripts appear in full in PDF format accompanied by an HTML abstract. "Just Accepted" manuscripts have been fully peer reviewed, but should not be considered the official version of record. They are accessible to all readers and citable by the Digital Object Identifier (DOI®). "Just Accepted" is an optional service offered to authors. Therefore, the "Just Accepted" Web site may not include all articles that will be published in the journal. After a manuscript is technically edited and formatted, it will be removed from the "Just Accepted" Web site and published as an ASAP article. Note that technical editing may introduce minor changes to the manuscript text and/or graphics which could affect content, and all legal disclaimers and ethical guidelines that apply to the journal pertain. ACS cannot be held responsible for errors or consequences arising from the use of information contained in these "Just Accepted" manuscripts.



ACS Publications

Biochemistry is published by the American Chemical Society, 1155 Sixteenth Street N.W., Washington, DC 20036

Published by American Chemical Society. Copyright © American Chemical Society. However, no copyright claim is made to original U.S. Government works, or works produced by employees of any Commonwealth realm Crown government in the course of their duties.

1  
2  
3  
4  
5  
6  
7  
8  
9  
10  
11  
12  
13  
14  
15  
16  
17  
18  
19  
20  
21  
22  
23  
24  
25  
26  
27  
28  
29  
30  
31  
32  
33  
34  
35  
36  
37  
38  
39  
40  
41  
42  
43  
44  
45  
46  
47  
48  
49  
50  
51  
52  
53  
54  
55  
56  
57  
58  
59  
60

The Stereochemical Consequences of Vinylpyruvate Hydratase-catalyzed Reactions

**REVISED June 29, 2016**

William H. Johnson, Jr.<sup>‡</sup>, Tyler M.M. Stack<sup>§</sup>, Stephanie M. Taylor<sup>§</sup>, Elizabeth A. Burks<sup>‡</sup>, and  
Christian P. Whitman<sup>‡,\*</sup>

Division of Chemical Biology and Medicinal Chemistry, College of Pharmacy, and Department  
of Molecular Biosciences, University of Texas, Austin, TX 78712

<sup>‡</sup>Division of Chemical Biology and Medicinal Chemistry

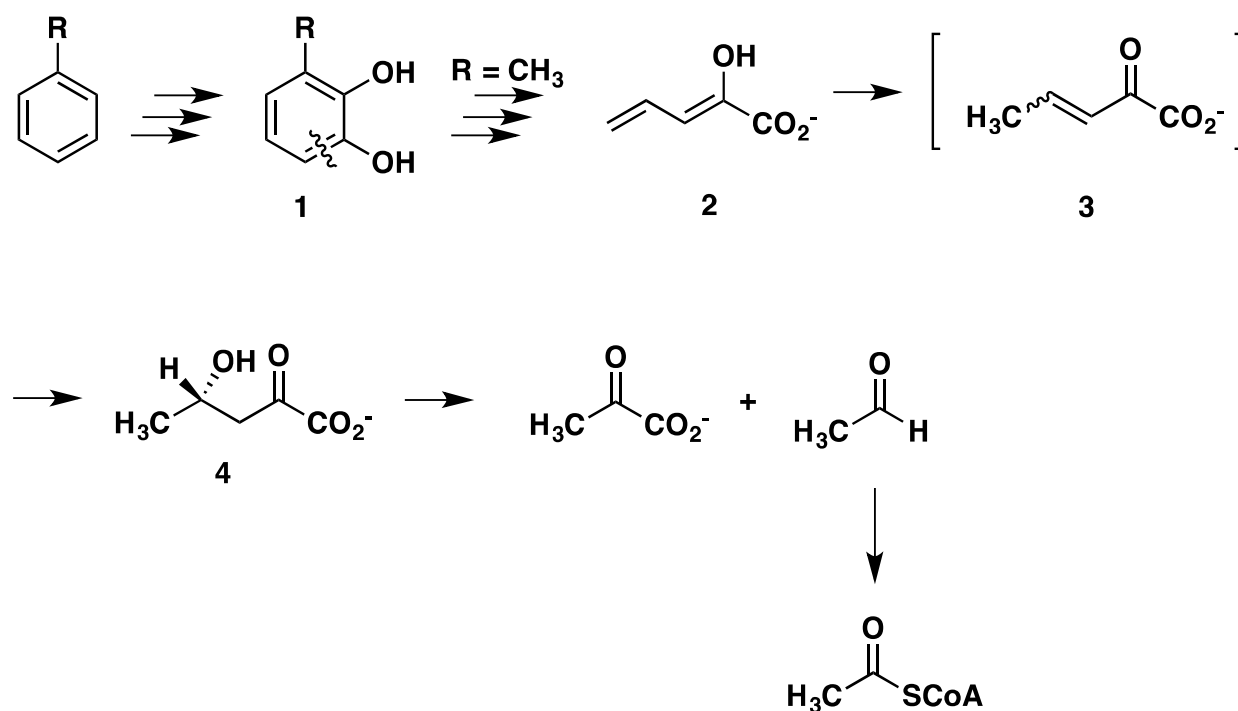
<sup>§</sup>Department of Molecular Biosciences

**ABSTRACT**

A stereochemical analysis has been carried out on two vinylpyruvate hydratases (VPH), which convert 2-hydroxy-2,4-pentadienoate to 2-keto-4*S*-hydroxypentanoate in meta-fission pathways. Bacterial strains with this pathway can use aromatic compounds as sole sources of energy and carbon. The analysis was carried out using the 5-methyl and 5-chloro derivatives of 2-hydroxy-2,4-pentadienoate with the enzymes from *Pseudomonas putida* mt-2 (Pp) and *Leptothrix cholodnii* SP-6 (Lc). In both organisms, VPH is in a complex with the preceding enzyme in the pathway, 4-oxalocrotonate decarboxylase (4-OD). In D<sub>2</sub>O, a deuteron is incorporated stereospecifically at the C-3 and C-5 positions of product by both Pp and Lc enzymes. Accordingly, the complexes generate (3*S*,5*S*)-3,5-[di-D]-2-keto-4*S*-hydroxyhexanoate and (3*S*,5*R*)-3,5-[di-D]-2-keto-4*R*-hydroxy-5-chloropentanoate (4*R* and 5*R* due to a priority numbering change). The substitution at C-5 (CH<sub>3</sub> or Cl) or the source of the enzyme (Pp or Lc) does not change the stereochemical outcome. One mechanism that can account for the results is the ketonization of the 5-substituted dienol to the  $\alpha,\beta$ -unsaturated ketone (placing a deuteron at C-5 in D<sub>2</sub>O), followed by the conjugate addition of water (placing a deuteron at C-3). The stereochemical outcome for VPH (from Pp and Lc) is the same as that reported for a related enzyme, 2-oxo-hept-4-ene-1,7-dioate hydratase, from *Escherichia coli* C. The combined observations suggest similar mechanisms for these three enzymes that could possibly be common to this group of enzymes.

Bacterial *meta*-fission pathways convert monocyclic aromatic compounds to useful cellular intermediates via catechol intermediates.<sup>1</sup> Catechol (**1**, Scheme 1) or a substituted derivative undergoes a signature *meta*-fission ring opening reaction, shown in Scheme 1, to generate a compound that is processed through a series of reactions to 2-hydroxy-2,4-pentadienoate (**2**, Scheme 1), or a derivative.<sup>2,3</sup> A metal-dependent ( $\text{Mn}^{2+}$  or  $\text{Mg}^{2+}$ ) hydratase then converts **2** to 2-keto-4*S*-hydroxypentanoate (**4**), most reasonably by the conjugate addition of water to the intermediate, 2-keto-3-pentenoate (**3**).<sup>2-6</sup> Subsequently, the product undergoes an enzyme-catalyzed retro-aldol cleavage to yield pyruvate and acetaldehyde. The aldolase is tightly associated with a dehydrogenase that uses  $\text{NAD}^+$  and CoASH to produce acetyl-CoA from acetaldehyde.<sup>7,8</sup> In this manner, pyruvate and acetyl-CoA are generated from aromatic compounds.

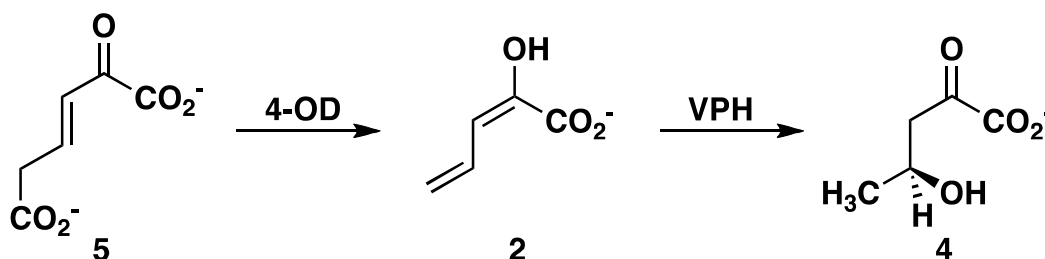
Scheme 1



Several hydratases have been identified, purified, and studied in some detail.<sup>2-6,9,10</sup> One, designated vinylpyruvate hydratase (EC 4.2.1.80; VPH<sup>1</sup>) from *Pseudomonas putida* mt-2, is part

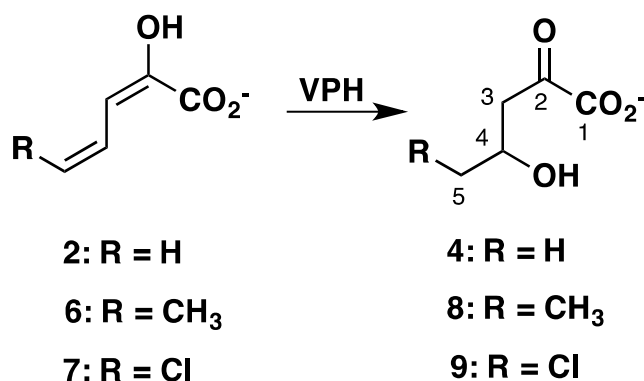
of an inducible pathway encoded by the TOL plasmid pWW0 that enables selected bacterial strains to use toluene, *m*- and *p*-xylene, 3-ethyltoluene, and 1,2,4-trimethylbenzene as their sole sources of carbon and energy.<sup>2,3</sup> VPH functions in a complex with the preceding enzyme in the pathway, 4-oxalocrotonate decarboxylase (4-OD), and the 4-OD/VPH complex converts 2-keto-3*E*-hexenedioate (**5**, Scheme 2) to **4**. A stereochemical analysis of the reaction (using a complex where VPH is nearly inactive) suggests that 4-OD converts **5** to **2** and that VPH, in turn, converts **2** to **4**.<sup>9</sup>

**Scheme 2**



Although VPH and other hydratases have been studied periodically over the last 35 years, our understanding of their mechanisms is far from complete.<sup>2-6,9-12</sup> The accumulated evidence implicates the mechanism shown in Scheme 1 where **2** initially undergoes an enzyme-catalyzed ketonization to produce **3**, which is then attacked by water at C-4. Protonation at C-3 completes the conjugate addition of water. The experimental evidence argues against a Schiff base mechanism,<sup>4</sup> and suggests the involvement of a metal-ion activated water molecule.<sup>4,5,10-12</sup> Although the mechanism is reasonable, incubation of the *trans* isomer of **3** with the enzyme does not afford product.<sup>4,5,11</sup> The chemical incompetence of *trans*-**3** raises three possibilities: the *cis*-isomer of **3** is the intermediate, various factors hamper the dissociation of the enzyme-bound intermediate and its re-association with the enzyme once free in solution, or the mechanism is not correct.<sup>4</sup>

Scheme 3



In this work, we report a stereochemical analysis of two VPH-catalyzed reactions using 5-methyl- and 5-chloro-2-hydroxy-2,4-pentadienoate (4Z-**6** and 4Z-**7**, respectively in Scheme 3), and the enzymes from *P. putida* mt-2 and *Leptothrix cholodnii* SP-6 (designated Pp and Lc, respectively). The analysis showed that the reactions produce the 4*S* isomers of **4** (in accord with previous work) and **8**, and the 4*R* isomer of **9** (due to a priority numbering change). When the same reactions are carried out in D<sub>2</sub>O, products **8** and **9**, are stereospecifically labeled at C-3 and C-5 with deuterium. Both deuterons are incorporated on the opposite face to that of the C-4 hydroxy group. The Pp and Lc enzymes show the same stereochemical result indicating that the presence of the substituent does not change the mechanism. These results are consistent with the enzyme-catalyzed ketonization of the dienol (i.e., **6** or **7**) to place a deuterium at C-5 for **8** and **9**, respectively, followed by the *anti* addition of water to incorporate deuterium at C-3 of the α,β-unsaturated ketone (with the *trans*-configuration). If the α,β-unsaturated ketone has the *cis*-configuration, then ketonization of the dienol would be followed by the *syn* addition of water. Nonetheless, both scenarios implicate the α,β-unsaturated ketone (i.e., **3** in Scheme 1) in the VPH reaction mechanism.

## EXPERIMENTAL PROCEDURES

*Materials.* Chemicals, biochemicals, buffers, solvents, and the components for Luria-Bertani (LB) media were obtained from sources reported elsewhere.<sup>13</sup> The syntheses of 2-hydroxy-2,4-pentadienoate (**2**) is reported elsewhere.<sup>9</sup> The 5-methyl derivative (**6**) was generated from 5-(methyl)-2-hydroxymuconate<sup>14</sup> following the procedure used to produce **2**.<sup>9</sup> The Phenyl Sepharose 6 Fast Flow, DEAE-Sepharose resins, and the prepacked PD-10 Sephadex G-25 columns were obtained from GE Healthcare (Piscataway, NJ). The Econo-Column chromatography columns and Freeze 'N Squeeze units were obtained from Bio-Rad Laboratories, Inc. (Hercules, CA). Enzymes and reagents used for molecular biology procedures were obtained from New England Biolabs, Inc. (Ipswich, MA). 5-(carboxymethyl)-2-Hydroxymuconate isomerase (CHMI),<sup>15</sup> 4-oxalocrotonate tautomerase (4-OT)<sup>16,17</sup>, 4-OD/VPH and 4-OD/E106QVPH from *P. putida* mt-2 were purified by procedures reported elsewhere with some modifications.<sup>9</sup> The 4-OD/VPH complex from *L. cholodnii* SP-6 was purified similarly to the *P. putida* mt-2 complex.<sup>9</sup> Activities were determined using previously described assays.<sup>9,15-17</sup>

*Bacterial Strains, Plasmids, and Growth Conditions.* *Escherichia coli* strains BL21-Gold(DE3), C41(DE3), and the DH5 $\alpha$  cells were obtained from Agilent Technologies (Santa Clara, CA), Lucigen (Middleton, WI), and Invitrogen (Carlsbad, CA), respectively. *L. cholodnii* SP-6 was a gift from Dr. David Emerson (Bigelow Laboratory for Ocean Sciences, East Boothbay, ME). The isolation of genomic DNA from *L. cholodnii* SP-6 cells was carried out by a procedure described elsewhere.<sup>18</sup> The pET vectors were obtained from Novagen (Madison, WI). Plasmids were isolated using the Sigma GenElute Plasmid Miniprep Kit, following the manufacturer's directions.

*General Methods.* Techniques for restriction enzyme digestion, ligation, transformation, and other standard molecular biology manipulations were based on methods described elsewhere<sup>19</sup>. All PCR reactions were carried out in a GeneAmp 2700 thermocycler (Applied Biosystems, Foster City, CA). Oligonucleotide primers were synthesized by Sigma-Aldrich. DNA sequencing was performed at the DNA core facility of the Institute of Cellular and Molecular Biology (ICMB) at the University of Texas at Austin. Mass spectral data were obtained on an LCQ electrospray ion-trap mass spectrometer (Thermo, San Jose, CA) in the ICMB Protein and Metabolite core facility. The samples were prepared as described previously.<sup>20</sup> Kinetic data were obtained at 24°C on an Agilent 8453 diode-array spectrophotometer. Nonlinear regression data analysis was performed using Grafit (Erithacus Software Ltd., Staines, U.K.) obtained from Sigma-Aldrich. Protein concentrations were determined by the Waddell method.<sup>21</sup> 4-OT was analyzed using tricine sodium dodecyl sulfate-polyacrylamide gel electrophoresis (SDS-PAGE) on 15% gels.<sup>22</sup> All other proteins were analyzed using Tris-glycine SDS-PAGE on 12% gels.<sup>23</sup> Gels were run on a Bio-Rad Mini-Protean II gel electrophoresis apparatus. Nuclear magnetic resonance (NMR) spectra were recorded on a Varian Unity+ 300 MHz or a Varian DirectDrive 600 MHz spectrometer (Palo Alto, CA), as noted. NMR signals were analyzed using the software program SpinWorks 3.1.6 (Copyright © 2009 Kirk Marat, University of Manitoba).

*Synthesis of 5-(chloro)-2-Hydroxy-2,4-hexadiene-1,6-dioate (12).* The protocol for the synthesis of **12** (Scheme 4) was based on the one used to generate 2-hydroxymuconate (**10**) except ethyl crotonate was replaced with ethyl 2-chlorocrotonate<sup>24</sup>. The ethyl-2-chlorocrotonate was generated as follows. Over a 1 h period, chlorine gas was streamed over a solution of ethyl crotonate (18.4 g, 161 mmol) dissolved in CCl<sub>4</sub> (100 mL) and DMF (2 drops). The reaction was carried out in a stoppered 500 mL round bottom flask. The solution was stirred at room



temperature overnight. Solvent was then removed and the residue distilled. Fractions boiling at 176-182°C were collected to yield 15.9 g of product. <sup>1</sup>H NMR analysis showed that it was mostly ethyl 2,3-dichlorobutyrates with a trace of ethyl 2-chlorocrotonate. In order to convert the remaining ethyl 2,3-dichlorobutyrates to ethyl 2-chlorocrotonate, the product mixture was dissolved in acetone (150 mL) in a 500 mL round bottom flask. Potassium carbonate (20 g) was added and the solution was allowed to gently reflux for 3 days. After cooling, the solid was filtered off and rinsed with ethyl acetate. The solvent was removed *in vacuo* and the residue purified by flash column chromatography (8:1 hexane/ethyl acetate). Fractions containing the desired product were combined and evaporated to dryness. The residue was used without further purification. <sup>1</sup>H NMR analysis showed an *E/Z* mixture of ethyl 2-chlorocrotonate, where the *E*-isomer predominates. Sodium metal (0.8 g, 1 eq) was allowed to react completely with ethanol (50 mL) and then 300 mL of toluene was added. The resulting solution was distilled (to remove water and ethanol) under an argon atmosphere until the temperature climbed above 80°C. The sodium ethoxide solution was then cooled in an ice bath and diethyl oxalate (4.9 g, 33.6 mmol), followed by ethyl 2-chlorocrotonate (5 g, 33.7 mmol) was added. This mixture was equilibrated to room temperature and stirred for 4 days. The bright yellow solid that precipitated was filtered, washed with hexane, and air-dried to yield 4.23 g. The solid (3.84 g, 11 mmol) was suspended in water (100 mL) and cooled in an ice bath. A 1 M solution of sodium hydroxide (32 mL, 32 mmol) was added dropwise over 30 min, and the reaction mixture was allowed to equilibrate to room temperature overnight. The dark yellow solution was cooled in an ice bath and concentrated phosphoric acid was added dropwise to adjust the pH to ~1.8. The solid that precipitated was filtered, air dried, and then crystallized from ethyl acetate to yield 1.91 g of 4Z-

**12.**  $^1\text{H}$  NMR ( $\text{CD}_3\text{OD}$ , 300 MHz)  $\delta$  6.50 (1H, d,  $J$  = 11.7 Hz), 7.94 (1H, d,  $J$  = 11.7 Hz);  $^{13}\text{C}$  NMR ( $\text{CD}_3\text{OD}$ , 75 MHz)  $\delta$  105.6, 124.3, 132.7, 149.8, 165.9, 166.4.

*Enzymatic Synthesis of 5-(chloro)-2-Hydroxy-2,4Z-pentadienoate (7) using 4-OD/E106QVPH (from P. putia mt-2).* The generation and isolation of **7** (Scheme 4) was based on the one used to generate **2** with the following modifications.<sup>9</sup> Accordingly, 4Z-**12** (1.0 mmol) was suspended in 100 mM  $\text{Na}_2\text{HPO}_4$  buffer (25 mL) that contained 3 mM  $\text{MgCl}_2$ . The pH was adjusted with 1 M NaOH to 7.2. To this solution, 5-(carboxymethyl)-2-hydroxymuconate isomerase, (250  $\mu\text{L}$  of a 3.4 mg/mL solution) was added and allowed to react for 5 min before adding 4OD/E106QVPH complex from *P. putida* mt-2 (2.5 mL of 1.2 mg/mL solution). The reaction mixture was monitored by UV, and when the peak at 304 nm no longer changed ( $\sim 20$  min), it was quenched by adjusting the pH to  $\sim 1.8$ -2.0 with 8.5% phosphoric acid. Extraction with ethyl acetate and further purification steps were carried out as reported previously<sup>9</sup>. (4Z)-**7**:  $^1\text{H}$  NMR ( $\text{DMSO}-d_6$ , 600 MHz)  $\delta$  6.31 (1H, H3, dd,  $J$  = 11.2 Hz, 1.1 Hz), 6.34 (1H, H5, dd,  $J$  = 7.1 Hz, 1.1 Hz), 6.75 (1H, H4, dd,  $J$  = 7.1 Hz, 11.3 Hz);  $^{13}\text{C}$  NMR ( $\text{CD}_3\text{OD}$ , 75 MHz)  $\delta$  105.6, 120.6, 124.7, 144.8, 167.2. In order to verify that the 4Z-isomer of **7** was generated, compound **12** was subjected to thermal decarboxylation, as described elsewhere.<sup>25</sup> Thermal decarboxylation yields a mixture of isomers.<sup>25</sup> (4E)-**7**:  $^1\text{H}$  NMR ( $\text{DMSO}-d_6$ , 600 MHz)  $\delta$  6.13 (1H, H3, dd,  $J$  = 11.1 Hz), 6.68 (1H, H5, dd,  $J$  = 13.3 Hz), 6.75 (1H, H4, dd,  $J$  = 11.1 Hz, 13.3 Hz).

*Cloning of L. cholodnii SP-6 4-OT.* A 50  $\mu\text{L}$  PCR reaction was set up that contained genomic DNA (480 ng), dNTPs (0.2 mM), Vent polymerase (0.5 unit), 10 $\times$  buffer (when diluted to 1 $\times$  contributes 2 mM  $\text{MgSO}_4$ ), and forward (5'-TAGTAGTAGCATATGCCCTTTGCCCAG-3') and reverse (5'-GATGATGATCTCGAGTCATTATTAGCGTCCGAG-3') primers (0.4  $\mu\text{M}$  each), where the restriction enzyme sites are underlined (*Nde*I and *Xho*I). The PCR amplification

protocol consisted of an initial 5-min denaturation cycle at 94° C, followed by 29 cycles of 94 °C for 1 min, 55 °C for 2 min, and 72 °C for 3 min, a 10-min elongation cycle at 72 °C, and ending with a hold at 4 °C. The reaction produced a DNA piece of the correct size that was eluted from a 1% agarose gel and processed through a Freeze 'N Squeeze unit. The liquid that was recovered was used as the template DNA for subsequent amplification in which four reactions (50 µL each) were set up. Each reaction contained 1 µL of the template DNA along with the components listed above. The PCR amplification protocol was identical to the one above except it began with a 2-min denaturation cycle. The reaction product was recovered from an agarose gel using a Freeze 'N Squeeze unit followed by ethanol precipitation of the DNA. The PCR product was inserted between the *NdeI* and *XhoI* restriction sites of a modified pET24a vector (the *BglII* restriction site was removed) following procedures described elsewhere.<sup>19</sup> The ligation product was used to transform *E. coli* DH5α cells by electroporation using a Bio-Rad MicroPulser Electroporation unit. The transformation reaction mixture was plated on LB/Kn (30 µg/mL) plates and the cells were grown overnight at 37° C. Following PCR screening, a positive colony was identified and used for the generation of additional plasmid for sequencing and protein expression.

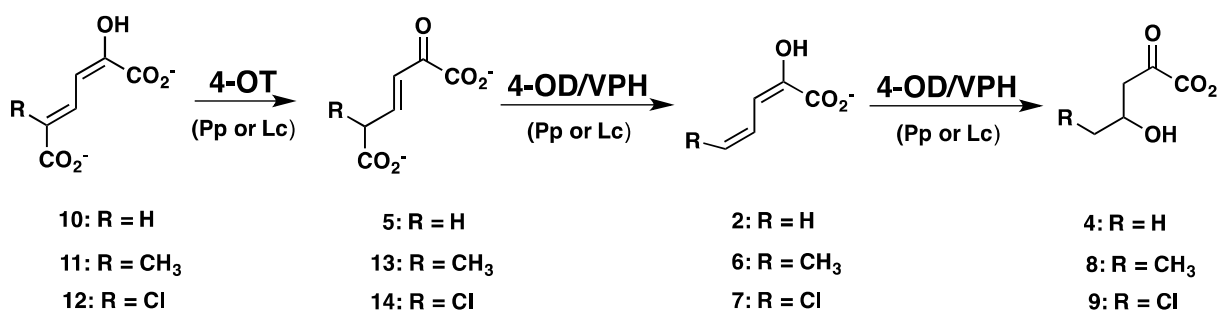
*Construction of the L. cholodnii SP-6 4-OD/VPH Expression Vector.* The 4OD/VPH complex from *L. cholodnii* SP-6 was cloned from genomic DNA, using the following primers. For the 4-OD gene, 5'-TAGTAGTAGCATATGGCACTGAATCGCACCG-3' was used as the forward primer and 5'-GATGATGATAAGCTTTCATTATTAGACGAAACGCATCGACAC-3' was used as the reverse primer (where the *NdeI* and *HindIII* restriction sites are underlined). For the VPH gene, 5'-TAGTAGTAGCATATGGACGCACTCACCATCC-3' was used as the forward primer and 5'-GATGATGATGGATCCTCATTATTAAATAAACCGCACCGACG-3'

was used as the reverse primer (where the *Nde*I and *Bam*HI restriction sites are underlined). For the initial PCR of each gene from genomic DNA, three reactions (50  $\mu$ L each) were prepared where each reaction contained genomic DNA (0.5  $\mu$ g), the accompanying 10 $\times$  buffer (5  $\mu$ L), 10 mM dNTPs (1  $\mu$ L), 2.5  $\mu$ L bovine serum albumin (10 mg/mL), Vent DNA polymerase (0.5 units), the forward and reverse primers (2  $\mu$ L each), and varying amounts of MgSO<sub>4</sub> in distilled H<sub>2</sub>O. Reactions were subjected to the PCR protocol described for the cloning of the Lc 4-OT gene. PCR reactions were eluted on 1% agarose gels. Bands of the correct size were excised, isolated using the Freeze 'N Squeeze units, and the product was used as template DNA in future reactions, following the same protocol. The PCR product and pET24a were then treated with the appropriate restriction enzymes (*Nde*I and *Hind*III for the 4-OD construct and *Nde*I and *Bam*HI for the VPH construct), ligated, and processed as described in the previous section to construct separate plasmids containing each gene (pET24a-4OD and pET24a-VPH).

In order to insert the 4-OD gene after VPH in the pET24a-VPH vector, an additional forward primer, 5'-TAGTAGTAGGGGATCCAGAAGGAGATATACATGGCACTGAATCGCACCG-3', was used (where the *Bam*HI restriction site is underlined). Accordingly, the PCR was repeated as described above using this primer (and the reverse primer used to synthesize the 4-OD gene) and pET24a-4OD as the PCR template. The PCR amplification protocol consisted of an initial 2-min denaturation cycle at 94 $^{\circ}$  C, followed by 29 cycles of 94  $^{\circ}$ C for 1 min, 55  $^{\circ}$ C for 1 min, and 72  $^{\circ}$ C for 3 min, a 10-min elongation cycle at 72  $^{\circ}$ C, and ending with a hold at 4  $^{\circ}$ C. The pET24a vector containing the VPH gene and the PCR product containing the 4-OD sequence with the *Bam*HI restriction site as well as a ribosome binding site and TATA box were treated with *Hind*III and *Bam*HI and processed as described above to construct a plasmid containing both genes.

Generation and Isolation of 3-Hydroxybutyrate (**15**), 3-Hydroxypentanoate (**16**), and 3-Hydroxy- $\gamma$ -butyrolactone (**17**). The VPH products (i.e., **4**, **8**, and **9**, Scheme 4) were generated from 2-hydroxymuconate (**10**, Scheme 4), 5-methyl-2-hydroxymuconate (**11**), and 5-chloro-2-hydroxymuconate (**12**) using 4-OT (Pp 4-OT: 6.7 mg/mL; Lc 4-OT: 1 mg/mL) and 4-OD/VPH (Pp 4-OD/VPH: 2.1 mg/mL; Lc 4-OD/VPH: 0.8 mg/mL). Each substrate (~32 mg of **10**, **11**, or **12**) was processed to its VPH product (**4**, **8**, or **9**, respectively).

Scheme 4



For each reaction, the substrate was dissolved in 100 mM Na<sub>2</sub>HPO<sub>4</sub> buffer, pH 9 (~4.8 mL). The pH was adjusted to ~7.0 with 2 M NaOH (~10  $\mu$ L) and an aliquot (10  $\mu$ L) of the Pp or Lc 4-OT was added. The solutions were then distributed evenly into 8 test tubes (~0.6 mL each) and aliquots of 4-OD/VPH (50  $\mu$ L of Pp or Lc in 10 mM NaH<sub>2</sub>PO<sub>4</sub> buffer containing 5 mM MgCl<sub>2</sub>) were added to the individual tubes. Aliquots were removed from representative tubes at ~10-min intervals and the UV absorbance was measured. The reactions were judged to be complete (~30-90 min) by the absence of significant UV absorbance between 220-300 nm. Hydrogen peroxide (~60  $\mu$ L of a 30% solution) was added to each reaction mixture and the resulting mixture was allowed to incubate at room temperature for 1 h.<sup>2,4</sup> A solution of catalase (10 mg/mL) was made in 20 mM NaH<sub>2</sub>PO<sub>4</sub> buffer, and 5-10  $\mu$ L of this solution was added to each reaction.<sup>2,4</sup> After bubbling ceased (indicating H<sub>2</sub>O<sub>2</sub> was no longer present), the reaction mixtures were combined and the pH was adjusted to 1.8 with 8.5% H<sub>3</sub>PO<sub>4</sub> (for 3-hydroxybutyrate, **15**, and 3-

hydroxypentanoate, **16**, in Scheme 5). These solutions were saturated with NaCl and extracted with ethyl acetate (3× ~25 mL). The ethyl acetate layers were combined and dried over anhydrous Na<sub>2</sub>SO<sub>4</sub>. After evaporation to dryness, the residue was dissolved in a small amount of ethyl acetate and purified by flash chromatography eluting with ethyl acetate. Yields were ~7.8 and 1.8 mg for **15** and **16**, respectively. For the generation of 3-hydroxy-γ-butyrolactone (**17**), the pH was not adjusted. The combined reaction mixtures were saturated with NaCl and extracted with ethyl acetate (3× ~25 mL). The residue was dissolved in a small amount of ethyl acetate and purified by flash chromatography (4:1 ethyl acetate: hexanes) to generate 4.2-5.5 mg of **17**. 3-Hydroxybutyric acid (**15**) <sup>1</sup>H NMR (CD<sub>3</sub>OH, 600 MHz) δ 1.19 (3H, d, *J* = 6.3 Hz), 2.37 (1H, dd, *J* = 5.6 Hz, 15.3 Hz), 2.41 (1H, dd, *J* = 7.4 Hz, 15.3 Hz), 4.14 (1H, m); <sup>13</sup>C NMR (CD<sub>3</sub>OH, 125 MHz) δ 23.3, 44.7, 65.6, 175.6. 3-Hydroxypentanoic acid (**16**) <sup>1</sup>H NMR (CD<sub>3</sub>OH, 600 MHz) δ 0.95 (3H, t), 1.50 (2H, m), 2.35 (1H, dd, *J* = 8.2 Hz, 15.3 Hz), 2.44 (1H, dd, *J* = 4.7 Hz, 15.3 Hz), 3.89 (1H, m); <sup>13</sup>C NMR (CD<sub>3</sub>OH, 125 MHz) δ 10.3, 31.0, 42.9, 70.9, 175.8. 3-Hydroxy-γ-butyrolactone (**17**) <sup>1</sup>H NMR (CD<sub>3</sub>OH, 600 MHz) δ 2.35 (1H, m), 2.80 (1H, dd, *J* = 5.9 Hz, 17.7 Hz), 4.20 (1H, m), 4.41 (1H, dd, *J* = 4.3 Hz, 10.0 Hz), 4.54 (1H, m); <sup>13</sup>C NMR (CD<sub>3</sub>OH, 125 MHz) δ 38.6, 68.4, 77.8, 179.1.

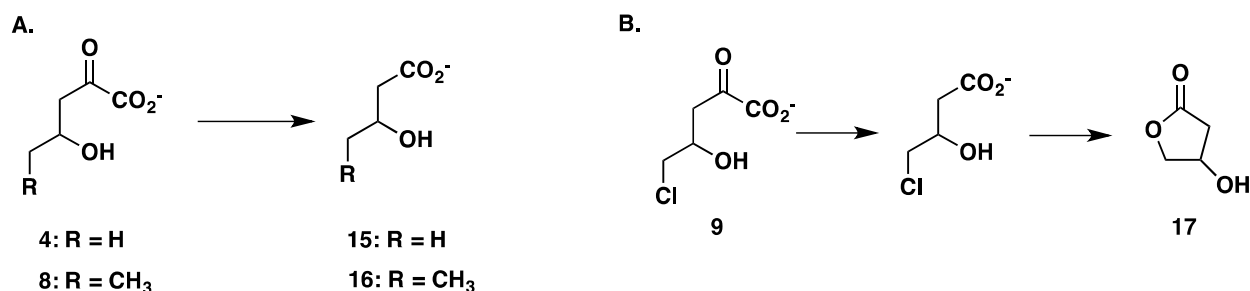
*Assignment of the Stereochemistry at C-3 of 3-Hydroxybutyrate (15), 3-Hydroxypentanoate (16), and 3-Hydroxy-γ-butyrolactone (17).* Samples were dissolved separately in methanol (**15** and **17**) or chloroform (**16**) and the optical rotations were measured using a Perkin Elmer 241 MC Polarimeter. Several readings were taken (~10) and averaged to produce the rotation that was used to calculate the reported specific rotations (Table 1). A specific rotation was also determined for the commercially available *S*-isomer of **15**.<sup>26</sup> The specific rotations for **16** and **17** were compared to those reported in the literature.<sup>27,28</sup>

*Assignment of the Stereochemistry at C-3 and C-5 of 8 and 9 by  $^1\text{H}$  NMR Spectroscopy.* The Pp and Lc 4-OD/VPH were exchanged into 100 mM  $\text{Na}_2\text{HPO}_4$  buffer, pH 7.2, or 100 mM  $\text{Na}_2\text{DPO}_4$  buffer, pH 7.2, where each buffer contained 5 mM  $\text{MgCl}_2$ . To an NMR tube was added 600  $\mu\text{L}$  of 100 mM  $\text{Na}_2\text{HPO}_4$  buffer or 100 mM  $\text{Na}_2\text{DPO}_4$  buffer (both at pH  $\sim 9$ ) along with 30  $\mu\text{L}$  of a solution of **6** (Scheme 3 to produce **8**) (16.8 mg) dissolved in  $\text{DMSO}-d_6$  (126  $\mu\text{L}$ ). The addition of substrate adjusted the pH to  $\sim 7$ . An initial  $^1\text{H}$  NMR spectrum of the reaction mixture was recorded before the addition of enzyme. After an aliquot of enzyme (25  $\mu\text{L}$  Pp or Lc 4-OD/VPH) was added, spectra were acquired every 3 min until the reaction was complete ( $\sim 20$  min) for the reactions run in 100 mM  $\text{Na}_2\text{HPO}_4$  buffer ( $\text{H}_2\text{O}$ ). This same series of  $^1\text{H}$  NMR experiments was repeated using 30  $\mu\text{L}$  of a solution of **7** (12.3 mg in 92  $\mu\text{L}$   $\text{DMSO}-d_6$ ) to produce **9** (Scheme 3). For the  $^1\text{H}$  NMR experiments carried out in  $\text{Na}_2\text{DPO}_4$  buffer ( $\text{D}_2\text{O}$ ), a single  $^1\text{H}$  NMR spectrum was recorded for both **8** and **9** in order to minimize the exchange at C-3 and C-5. **8**:  $^1\text{H}$  NMR ( $\text{NaH}_2\text{PO}_4$ , 600 MHz)  $\delta$  0.72 (3H, t), 1.33 (2H, m), 2.66 (1H, dd,  $J = 8.4$  Hz, 16.6 Hz), 2.75 (1H, dd,  $J = 4.2$  Hz, 16.6 Hz), 3.87 (1H, m). 3,5-di[D]**8**:  $^1\text{H}$  NMR ( $\text{NaD}_2\text{PO}_4$ , 600 MHz)  $\delta$  0.71 (3H, d,  $J = 7.4$  Hz), 1.30 (1H, m,  $J = 7.4$ -7.6 Hz), 2.64 (0.9H, d,  $J = 8.4$  Hz), 3.87 (1H, t). **9**:  $^1\text{H}$  NMR ( $\text{NaH}_2\text{PO}_4$ , 600 MHz)  $\delta$  2.84 (1H, dd,  $J = 7.8$  Hz, 17.4 Hz), 2.89 (1H, dd,  $J = 4.8$  Hz, 17.4 Hz), 3.45 (1H, dd,  $J = 5.8$  Hz, 11.6 Hz), 3.53 (1H, dd,  $J = 3.9$  Hz, 11.6 Hz), 4.21 (1H, m). 3,5-di[D]**9**:  $^1\text{H}$  NMR ( $\text{NaD}_2\text{PO}_4$ , 600 MHz)  $\delta$  2.82 (0.3H, d,  $J = 8.2$  Hz), 3.44 (0.8H, d,  $J = 5.7$  Hz), 4.19 (1H, m).

## RESULTS

Assignment of C-4 Stereochemistry of 3-Hydroxybutyrate (**15**), 3-Hydroxypentanoate (**16**), and 3-Hydroxy- $\gamma$ -butyrolactone (**17**). The stereochemistry at the C4 hydroxyl of 2-keto-4-hydroxypentanoate (**4**), 5-methyl-2-keto-4-hydroxypentanoate (**8**), and 5-chloro-2-keto-4-hydroxypentanoate (**9**) was determined by their respective enzymatic generation from **10**, **11**, and **12** (Scheme 4) and their subsequent chemical degradation to 3-hydroxybutyrate (**15**), 3-hydroxypentanoate (**16**), and 3-hydroxy- $\gamma$ -butyrolactone (**17**) (Schemes 5A and B). The chemical degradation is based on previous protocols and involves the oxidative decarboxylation of the VPH products (using  $\text{H}_2\text{O}_2$ ) and purification.<sup>2,4,29</sup> In the course of these reactions, the degradation product of **9** (Scheme 5B) cyclizes to lactone **17** with the loss of the chloride, but retains the stereochemistry at C-4 (of **9**).

Scheme 5



The optical rotations of the three samples (generated using the Pp and Lc enzymes) are shown in Table 1 along with those of the authentic (and configurationally known) compounds. In all cases, the optical rotations are positive. The *S* isomer of **15** and **16** has a positive rotation and the *R* isomer of **17** has a positive rotation. This indicates that the Pp and Lc enzymes generate 2-keto-4*S*-hydroxypentanoate (**4**) and 2-keto-4*S*-hydroxyhexanoate (**8**), and that neither the methyl group nor the enzyme alters the stereochemistry. The stereochemical outcome reported here for **4** agrees with previous work.<sup>2,4,29</sup> The positive rotation for **17** indicates that the



1  
2  
3 *R* isomer of **17** has been generated and that both enzymes produce 5-chloro-2-keto-4*R*-  
4 hydroxypentanoate (**9**).  
5  
6

7  
8 *<sup>1</sup>H NMR Spectroscopic Analysis of the Products Generated by Pp and Lc 4-OD/VPH Using 6*  
9 *and 7 in D<sub>2</sub>O.* The preceding analysis shows that the Pp and Lc 4-OD/VPHs introduce a chiral  
10 carbon at C4 of **4**, **8**, and **9**. Hence, the protons at C3 of **4**, **8**, and **9** are diastereotopic as are the  
11 protons at C5 of **8** and **9**. (The C5 methyl group of **4** is achiral.) These protons will present a  
12 complex set of signals in a <sup>1</sup>H NMR spectrum when the reactions are carried out in H<sub>2</sub>O. The  
13 stereoselective or stereospecific incorporation of deuterium will simplify the set of signals when  
14 the same reactions are carried out in D<sub>2</sub>O.  
15  
16  
17  
18  
19  
20  
21  
22  
23

24 A partial <sup>1</sup>H NMR spectrum corresponding to the fully protio **8** is shown in Figure 1A. The  
25 signals corresponding to the diastereotopic protons at C3 and C5 are indicated. Each  
26 diastereotopic proton at C3 appears as a doublet of doublets (centered at 2.66 ppm) with the  
27 downfield one centered at 2.75 ppm and the upfield one centered at 2.64 ppm. When the Pp  
28 reaction is carried out in D<sub>2</sub>O, there is a loss of the downfield doublet of doublets and the  
29 collapse of the upfield signal into a broadened doublet at 2.64 ppm (Figure 1B). The Lc reaction  
30 gives the same result (Figure 1C). (The doublet at 2.78 ppm, indicated by the asterisk in Figures  
31 1B and 1C, corresponds to the C3 methylene group of 2-oxo-4-hexenoate.)  
32  
33  
34  
35  
36  
37  
38  
39  
40  
41  
42

43 The two diastereotopic protons at C5 appear as a complex multiplet centered at 1.33 ppm  
44 (Figure 1A) due to coupling with the C4 proton and the additional coupling with the C6 methyl  
45 group (along with the germinal coupling of the C5 protons). When the Pp reaction is carried out  
46 in D<sub>2</sub>O, the signal simplifies into a broadened triplet-multiplet at (1.30 ppm). Again, the Lc  
47 reaction gives the same result (Figure 1C). (The doublet at 1.43 ppm, indicated by the asterisk  
48 in Figures 1B and 1C, corresponds to the C5 methyl group of 2-oxo-4-hexenoate.)  
49  
50  
51  
52  
53  
54  
55  
56  
57  
58  
59  
60

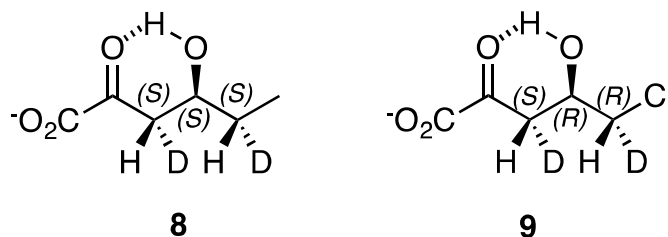
The same set of experiments was carried out using the Pp and Lc 4-OD/VPH with **7**. A partial  $^1\text{H}$  NMR spectrum corresponding to the fully protio **9** is shown in Figure 2A where the diastereotopic protons at C3 and C5 are indicated. Each diastereotopic proton at C3 appears as a doublet of doublets (centered at 2.87 ppm). When the Pp reaction is carried out in  $\text{D}_2\text{O}$ , there is a loss of the downfield doublet of doublet and a collapse of the upfield doublet of doublets into a broadened doublet centered at 2.82 ppm (Figure 2B). The Lc reaction in  $\text{D}_2\text{O}$  gives the same result (Figure 2C), indicating that the halogen or the enzymes does not change the stereochemical outcome.

In this case, the signals corresponding to the diastereotopic protons at C5 (of **9**) are shifted downfield. Each diastereotopic proton at C5 gives rise to a doublet of doublets (centered at 3.49 ppm) where the downfield signal is centered at 3.53 ppm and the upfield one is centered at 3.45 ppm (Figure 2A). When the Pp reaction is carried out in  $\text{D}_2\text{O}$ , there is a loss of the downfield doublet of doublet and a collapse of the upfield doublet of doublets into a broadened doublet centered at 3.44 (Figure 2B). The Lc reaction in  $\text{D}_2\text{O}$  gives the same result (Figure 2C), indicating that the halogen does not change the stereochemical outcome.

*Assignment of the Stereochemistry at C-3 and C-5 of **8** and **9**.* The stereochemistry at C3 of 3,5-di[D]**8** and 3,5-di[D]**9** can be assigned based on the coupling constants in the  $^1\text{H}$  NMR spectra (Figures 1B,C and 2B,C). We have previously shown the stereoselective incorporation of a deuteron at C-3 of **4**, and assigned the stereochemistry by chemical degradation and  $^1\text{H}$  NMR analysis of the resulting product.<sup>9,29</sup> These analyses showed that the 4-OD/VPH complex produces the (3*S*,4*S*)-[3-D]**4** in  $\text{D}_2\text{O}$ . A deuteron is also incorporated at C-5, but C-5 remains achiral. In the present analysis, we confirmed that the complex produces the 3*S* isomer of 3-[D]**8** and 3-[D]**9**. In both products, the vicinal coupling constant (8.4 and 8.2 Hz, respectively)

indicates an *anti* relationship between the remaining C-3 proton and the C-4 proton (due to the conformation stabilized by a hydrogen bond between the C-4 hydroxyl group and C-2 carbonyl oxygen<sup>11</sup>, as shown in Scheme 6).<sup>30</sup> For C-5 in **8** and **9**, the vicinal coupling constant (7.4 and 5.7 Hz, respectively) indicates an *anti* relationship between the remaining C-5 proton and the C-4 proton (assuming both molecules have a conformation stabilized by a hydrogen bond between the C-4 hydroxyl group and C-2 carbonyl oxygen<sup>11</sup>, as shown in Scheme 6).<sup>30</sup> In this case, the complex produces the 5*S* isomer of [5-D]**8** and the 5*R* isomer of [5-D]**9** (due to a change in priority). Hence, the 4-OD/VPH complex from *P. putida* mt-2 and *L. cholodnii* produced (3*S*,4*S*,5*S*)-3,5-[di-D]**8** and (3*S*,4*R*,5*R*)-3,5-[di-D]**9**.

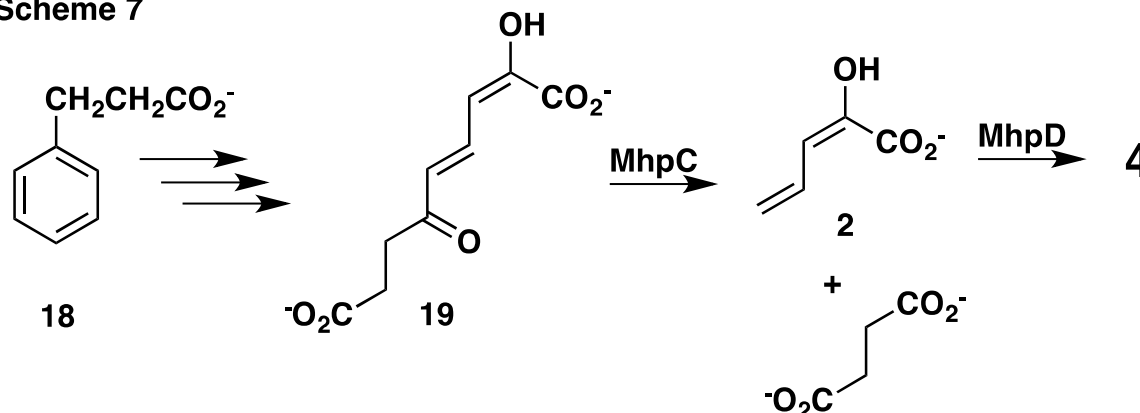
**Scheme 6**



## DISCUSSION

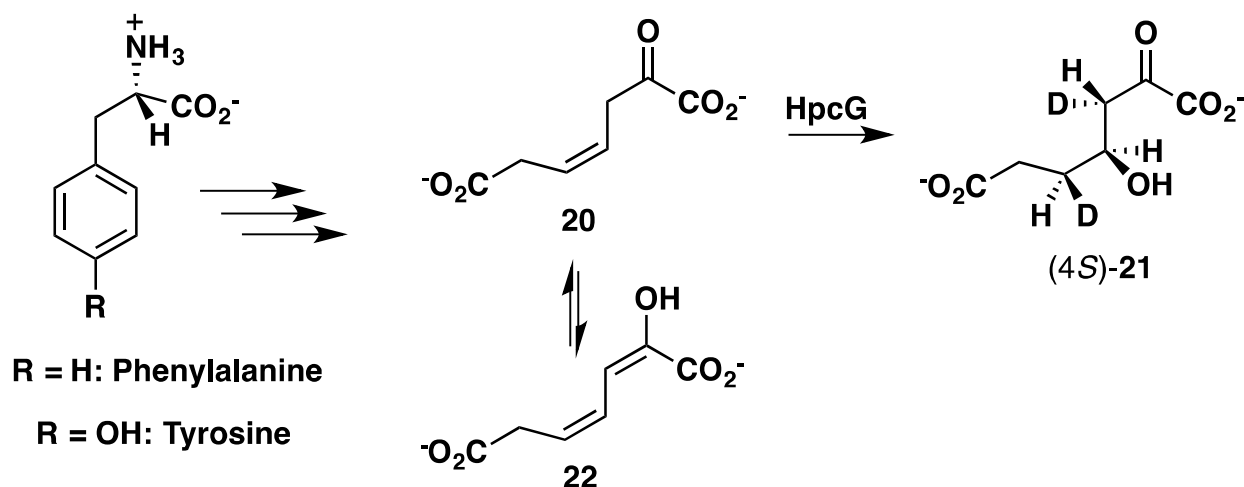
In addition to VPH from the TOL plasmid (pWW0), two other hydratases have been studied in detail.<sup>5,11,12</sup> The first, designated MhpD, catalyzes the same reaction in a strain of *E. coli* (*E. coli* str. K-12 substr. W3110) that degrades phenylpropionate (**18**, Scheme 7) via a meta-fission pathway.<sup>5</sup> MhpD does not exist as a complex with the preceding enzyme in the pathway, which is MhpC, a hydrolase that converts 2-hydroxy-6-ketonona-2,4-diene 1,9-dioate (**19**) to **2** and succinate. It has 42% sequence identity and 58% similarity with VPH (including the conservation of several regions of the sequence).<sup>5</sup>

**Scheme 7**



The second enzyme, 2-oxo-hept-4-ene-1,7-dioate hydratase (designated HpcG or OHED hydratase), converts 2-oxo-hept-4Z-ene-1,7-dioate (**20**, Scheme 8) to 2-oxo-4S-hydroxy-hepta-1,7-dioate (**21**) in the homoprotocatechuate (HPC) pathway in *E. coli* C.<sup>11,12</sup> The HPC pathway parallels the reactions of the catechol meta-fission pathway (Scheme 1), but the intermediates have a carboxymethyl group (i.e.,  $-\text{CH}_2\text{CO}_2^-$ ) at C-5 (of **2** and **4** in Scheme 1, for example). The pathway provides a degradative route for phenylalanine and tyrosine.<sup>11,12</sup> OHED hydratase functions as a “free-standing” enzyme that is not part of a complex.

Scheme 8



Studies of VPH have been complicated by the observation that the enzyme exists as a complex with 4-OD, the preceding enzyme in the pathway.<sup>3,4,9</sup> Both 4-OD and VPH from *P. putida* mt-2 are largely insoluble when expressed separately.<sup>3,9</sup> Nonetheless, a number of insights were obtained by studies of the complex (metal ion dependence where  $Mn^{2+}$  is preferred over  $Mg^{2+}$ , lack of a Schiff base or lactone intermediate, and the complex produces 4S-4) and the complex where each enzyme is inactivated by mutagenesis of key residues identified by sequence analysis. Studies of the 4-OD/E106QVPH complex (which is nearly devoid of hydratase activity) yielded two critical insights: Glu-106 is essential for catalysis by VPH, and **2** is the product of 4-OD and the likely substrate for VPH.<sup>9</sup>

These findings are largely consistent with those observed for MhpD and HpcG.<sup>5,11,12</sup> One apparent variation is that **20** appears to be the substrate for the OHED hydratase reaction, and not 2-hydroxy-2,4Z-heptadiene-1,7-dioate (**22**), the 5-carboxymethyl analog of **2**. This conclusion is based on the observation that the previous enzyme in the pathway, 5-(carboxymethyl)-2-oxo-3-hexene-1,6-dioate decarboxylase (COHED), produces 3-[D]**20** when the reaction is carried out in  $D_2O$ .<sup>25</sup> (The COHED-catalyzed reaction produces the 4Z-isomer of **20**, and the 4-OD-catalyzed

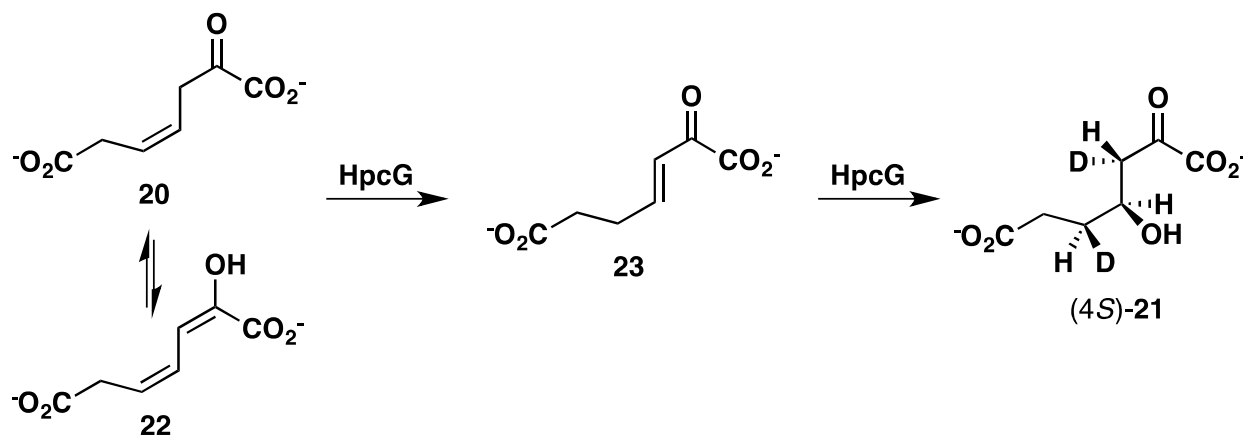
reaction produces the 4Z isomers of **6** and **7** from **13** or **14**, respectively.) However, **20** and **22** are in rapid equilibrium in aqueous buffer so a direct determination is not possible. A stereochemical analysis of the OHED hydratase-catalyzed reaction (in D<sub>2</sub>O) showed that the final product of the reaction is (3*S*,4*S*,5*S*)-3,5-[di-D]**21**.<sup>11</sup> [In the initial report, the stereochemical assignment was inadvertently switched at C-3 of (4*S*)-**21**].<sup>11</sup> The analysis clearly established that deuterons were incorporated at C3 and C5 in a stereospecific manner when the reaction was carried out in D<sub>2</sub>O. Any proposed mechanism would have to account for the involvement of both centers.

We (and others) have suggested a ketonization/hydration mechanism (for VPH) or an isomerization/hydration mechanism (for OHED hydratase). In these scenarios, water would be added by the enzyme to an  $\alpha,\beta$ -unsaturated ketone (**3** in Scheme 1).<sup>5,11,12</sup> In the VPH-catalyzed reaction, ketonization of **2** in D<sub>2</sub>O would label C-5 (of **3**) with deuterium. The addition of water (D<sub>2</sub>O) would then label C-3 (of product, **4**) with deuterium. Various groups have proposed that the water would be activated by the metal ion.<sup>4,5,10-12</sup>

The strongest support for this mechanism comes from the crystallographic analysis of OHED hydratase carried out by Izumi et al.<sup>12</sup> Based on this analysis, the mechanism shown in Figure 3 was formulated. The authors suggested that the metal ion (Mg<sup>2+</sup>) is coordinated by the C-2 carbonyl group and the C-1 carboxylate group (of **20**) based on modeling the substrate into the crystal structure of the enzyme-oxalate complex.<sup>12</sup> (Oxalate is a competitive inhibitor of the enzyme.<sup>5</sup>) This coordination and a hydrogen bond to Lys-61 favor the enol form (**22**) of the substrate (**20**). A nearby water molecule (hydrogen bonded to Glu-106) is responsible for proton/deuteron exchange at C-3 (in D<sub>2</sub>O). The enol form then undergoes ketonization to form the  $\alpha,\beta$ -unsaturated ketone (e.g., **23**, Scheme 9) with incorporation of a deuteron at C-5. This

deuteron comes from a nearby water molecule held in place by the backbone carbonyl group of Ala-166 and the side chain carboxylate group of Asp-79. The loss of the proton from this water molecule is proposed to activate the water so it can add to C-4 (according to Izumi et al).<sup>12</sup> Hence, the deuteron at C-5 (in D<sub>2</sub>O) and the hydroxyl group at C-4 come from the same side (in the active site). The crystal structure further indicates that the water molecule is not one of those coordinated by the Mg<sup>2+</sup>, which argues against metal activated water molecule. Finally, the reaction is completed by the return of the deuteron at C-3 (from the water molecule hydrogen bonded to Glu-106). In this case, the addition of the hydroxyl group at C-4 and the deuteron at C-3 are on opposite sides (suggesting an *anti* addition).

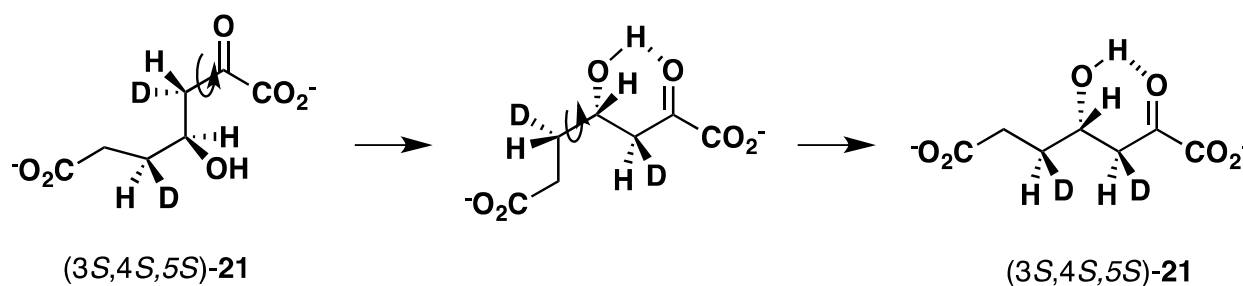
Scheme 9



Izumi et al. also provided an explanation for the observation that the  $\alpha,\beta$ -unsaturated ketone (in this case, 3E-23) is not processed by the enzyme when introduced exogenously.<sup>12</sup> The ketonization of 22 to 23 places a proton at C-5 (deuteron in D<sub>2</sub>O). Because this step activates the water molecule for attack at C-4, the water molecule would be in a much less reactive state to add to 23 when presented with 23.<sup>12</sup> Although 23 might bind to the enzyme, it would not be processed.<sup>12</sup> (The 3Z isomer of 23 puts the two carboxylate groups in an unfavorable conformation so that it is not a likely intermediate.<sup>11,12</sup>)

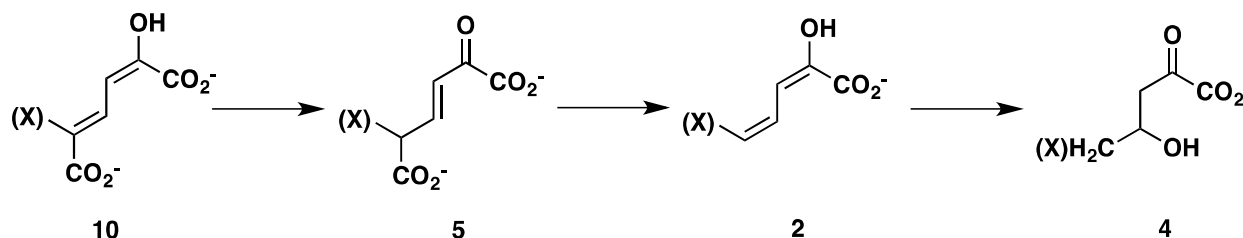
The two VPH-catalyzed reactions show the same stereochemical outcome as that of the OHED-catalyzed reaction. (When product **21** is released into solution, it adopts the more stable conformation as shown in Scheme 10.<sup>11</sup>) The same mechanism proposed by Izumi et al.<sup>12</sup> could be operative although the ketonization of **2** to **3** might not be a discrete step, but simply a delocalization of the electrons across the dienolate system. In fact, the mechanism might be a common one to this group of enzymes.

Scheme 10



Many more similar hydratases have been identified in the course of various sequencing projects. Among these hydratases is one that is proposed to process halogenated substrates in a meta-fission pathway in *Comamonas sp.* strain CNB-1.<sup>31,32</sup> *Comamonas sp.* strain CNB-1 utilizes 4-chloronitrobenzene as a sole carbon source.<sup>31,32</sup> The proposed degradative pathway parallels the canonical meta-fission pathway where the intermediates corresponding to **10**, **5**, **2**, and **4** are depicted with a halogen substituent at the X position (Scheme 11).

Scheme 11



The presence of the halogen raises questions about its effect on binding and reactivity and whether the corresponding enzymes from *C. sp.* strain CNB-1 have evolved the capability to



process the halogenated intermediates selectively over the non-halogenated ones.<sup>6,33</sup> However, the strain is not available. Although *L. cholodnii* SP-6 is not known for its ability to degrade halogenated aromatic compounds,<sup>34</sup> 4-OT, 4-OD, and VPH from *L. cholodnii* SP-6 share high pairwise sequence identity and similarity with the reported sequences for the *C.* strain CNB-1 (4-OT: 78%, 87%; 4-OD: 82%, 90%; VPH: 85%, 92%; identity and similarity, respectively). In contrast, the *P. putida* enzymes show lower sequence identity and similarity with the Lc enzymes (4-OT: 45%, 71%; 4-OD: 64%, 82%; VPH: 67%, 78%; identity and similarity, respectively). These similarities suggest that the Lc enzymes might be representative models for the unavailable *C. sp.* strain CNB-1 enzymes.

The effects of halogen substituents have been studied more extensively in polychlorinated biphenyl (PCB)-degrading organisms.<sup>33</sup> The studies were prompted by the observation that the bacteria can only partially degrade PCBs. Several roadblocks were uncovered, but they all have a steric basis. For example, one enzyme hydrolyzed a series of 3-substituted substrates in the order  $H > F > Cl > CH_3$ .<sup>33</sup> The larger the substituent, the less likely it was to be hydrolyzed. Large substituents also block the formation of a key intermediate and led to non-productive binding modes.<sup>33</sup>

Our study using **6** (where the 5-CH<sub>3</sub> might present a steric hindrance) and **7** (where the 5-Cl might present a steric and/or electronic impairment) as substrates for VPH indicates that there are no differences in the overall stereochemical outcomes. Although kinetic parameters have not been reported, this finding suggests that there are no major differences in the arrangement of the active site groups involved in the ketonization/hydration mechanism. In the course of this study, we found that the 5-halogenated-2-hydroxymuconates (e.g., **10** in Scheme 11 where R = Cl, Br, and F) behave very differently in solution than 2-hydroxymuconate (**10** where R = H). There

1  
2  
3  
4  
5  
6  
7  
8  
9  
10  
11  
12  
13  
14  
15  
16  
17  
18  
19  
20  
21  
22  
23  
24  
25  
26  
27  
28  
29  
30  
31  
32  
33  
34  
35  
36  
37  
38  
39  
40  
41  
42  
43  
44  
45  
46  
47  
48  
49  
50  
51  
52  
53  
54  
55  
56  
57  
58  
59  
60

were also subtle differences in the processing of these compounds by the Pp and Lc enzymes, with consequences for activity. These results will be reported in the near future.

**AUTHOR INFORMATION****Corresponding Author**

\*E-mail: whitman@austin.utexas.edu. Telephone: (512) 471-6198. Fax (512) 232-2606.

**Funding**

This research was supported by the National Institutes of Health Grants (GM-41239) and the Robert A. Welch Foundation Grant (F-1334).

**Notes**

The authors declare no competing financial interest.

1  
2  
3  
4  
5  
6  
7  
8  
9  
10  
11  
12  
13  
14  
15  
16  
17  
18  
19  
20  
21  
22  
23  
24  
25  
26  
27  
28  
29  
30  
31  
32  
33  
34  
35  
36  
37  
38  
39  
40  
41  
42  
43  
44  
45  
46  
47  
48  
49  
50  
51  
52  
53  
54  
55  
56  
57  
58  
59  
60

**ACKNOWLEDGEMENTS**

The protein mass spectrometry analysis was conducted in the Institute for Cellular and Molecular Biology Protein and Metabolite Analysis Facility at the University of Texas at Austin. We thank Steve D. Sorey (Department of Chemistry, University of Texas at Austin) for his expert assistance in the acquisition of the <sup>1</sup>H NMR spectra.

## ABBREVIATIONS

DMF, dimethyl formamide; DMSO- $d_6$ , dimethyl sulfoxide- $d_6$ ; Lc, *Leptothrix cholodnii* SP-6; LB, Luria-Bertani; MhpD, 2-hydroxypentadienoic acid hydratase; 4-OD, 4-oxalocrotonate decarboxylase; 4-OT, 4-oxalocrotonate tautomerase; PCB, polychlorinated biphenyl; PCR, polymerase chain reaction; Pp, *Pseudomonas putida* mt-2; SDS-PAGE, sodium dodecyl sulfate-polyacrylamide gel electrophoresis; VPH, vinylpyruvate hydratase

## REFERENCES

1. Harayama, S., and Rekik, M. (1990) The meta cleavage operon of TOL degradative plasmid pWW0 comprises 13 genes. *Mol. Gen. Genet.* 221, 113-120.
2. Collinsworth, W.L., Chapman, P.J., and Dagley, S. (1973) Stereospecific enzymes in the degradation of aromatic compounds by *Pseudomonas putida*. *J. Bacteriol.* 113, 922-931.
3. Harayama, S., Rekik, M., Ngai, K.-L., and Ornston, L. N. (1989) Physically associated enzymes produce and metabolize 2-hydroxy-2,4-dienoate, a chemically unstable intermediate formed in catechol metabolism via meta cleavage in *Pseudomonas putida*. *J. Bacteriol.* 171, 6251-6258.
4. Lian, H., and Whitman, C. P. (1994) Stereochemical and isotopic labeling studies of 4-oxalocrotonate decarboxylase and vinylpyruvate hydratase: Analysis and mechanistic implications. *J. Am. Chem. Soc.* 116, 10403-10411.
5. Pollard, J. R., and Bugg, T. D. H. (1998) Purification, characterization, and reaction mechanism of monofunctional 2-hydroxypentadienoic acid hydratase from *Escherichia coli*. *Eur. J. Biochem.* 251, 98-106.
6. Wang, P., and Seah, S.Y.K. (2005) Determination of the metal ion dependence and substrate specificity of a hydratase involved in the degradation pathway of biphenyl/chlorobiphenyl. *FEBS J.* 272, 966-974.
7. Manjasetty, B., Powlowski, J., and Vrielink, A. (2003) Crystal structure of a bifunctional aldolase-dehydrogenase: sequestering a reactive and volatile intermediate. *Proc. Natl. Acad. Sci. USA* 100, 6992-6997.

8. Baker, P., Pan, D., Carere, J., Rossi, A., Wang, W., and Seah, S.Y.K. (2009) Characterization of an aldolase-dehydrogenase complex that exhibits substrate channeling in the polychlorinated biphenyls degradation pathway. *Biochemistry* 48, 6551-6558.
9. Stanley, T. M., Johnson, W. H. Jr., Burks, E. A., Whitman, C. P., Hwang, C., and Cook, P. F. (2000) Expression and stereochemical and isotope effect studies of active 4-oxalocrotonate decarboxylase. *Biochemistry* 39, 718-726.
10. Johnson, Jr., W.H., Wang, S.C, Stanley, T.M., Czerwinski, R.M, Almrud, J.J., Poelarends, G.J., Murzin, A.G., and Whitman, C.P. (2004) 4-Oxalocrotonate tautomerase, its homologue YwhB, and active vinylpyruvate hydratase: synthesis and evaluation of 2-fluoro substrate analogs. *Biochemistry* 43, 10490-10501.
11. Burks, E. A., Johnson Jr., W.H., and Whitman, C.P. (1998) Stereochemical and isotopic labeling studies of 2-oxo-hept-4-ene-1,7-dioate hydratase: evidence for an enzyme-catalyzed ketonization step in the hydration reaction. *J. Am. Chem. Soc.* 120, 7665-7675.
12. Izumi, A., Rea, D, Adachi, T., Unzai, S, Park, S.-Y., Roper, D.I., and Tame, J.R.H. (2007) Structure and mechanism of HpcG, a hydratase in the homoprotocatechuate degradation pathway of *Escherichia coli*. *J. Mol. Biol.* 370, 899-911.
13. Burks, E.A., Yan, W., Johnson, Jr., W.H., Li, W., Schroeder, G.K., Min, C., Gerratana, B., Zhang, Y., and Whitman, C.P. (2011) Kinetic, crystallographic, and mechanistic characterization of TomN: elucidation of a function for a 4-oxalocrotonate tautomerase homologue in the tomaymycin biosynthetic pathway. *Biochemistry* 35, 7600-7611.
14. Lian, H., Czerwinski, R. M., Stanley, T. M., Johnson Jr., W. H., Watson, R.J., and Whitman, C.P. (1998) The contribution of the substrate's carboxylate group to the mechanism of 4-oxalocrotonate tautomerase. *Bioorg. Chem.* 26, 141-156.

15. Hajipour, G., Johnson, W. H., Jr., Dauben, P. D., Stolowich, N. J., and Whitman, C. P. (1993) Chemical and enzymatic ketonization of 5-(carboxymethyl)-2-hydroxymuconate. *Biochemistry* 115, 3533-3542.
16. Burks, E.A., Fleming, C.D., Mesecar, A.D., Whitman, C.P., and Pegan, S.D. (2010) Kinetic and structural characterization of a heterohexamer 4-oxalocrotonate tautomerase from *Chloroflexus aurantiacus* J-10-fl: implications for functional and structural diversity in the tautomerase superfamily. *Biochemistry* 49, 5016-5027
17. Poelarends, G.J., Almrud, J.J., Serrano, H., Darty, J.E., Johnson, Jr., W.H., Hackert, M.L., and Whitman, C.P. (2006) Evolution of enzymatic activity in the tautomerase superfamily: Mechanistic and structural consequences of the L8R mutation in 4-oxalocrotonate tautomerase. *Biochemistry* 45, 7700-7708
18. Pospiech, A., and Neumann, B. (1995) A versatile quick-prep of genomic DNA from Gram-positive bacteria. *Trends in Genetics* 11, 217-218.
19. Sambrook, J., Fritsch, E. F., and Maniatis, T. (1989) *Molecular cloning: A laboratory manual*, 2nd ed., Cold Spring Harbor Laboratory Press, Plainview, NY.
20. Wang, S. C., Person, M. D., Johnson, W. H. Jr., and Whitman, C. P. (2003) Reactions of *trans*-3-chloroacrylic acid dehalogenase with acetylene substrates: Consequences of and evidence for a hydration reaction. *Biochemistry* 42, 8762-8773.
21. Waddell, W.J. (1956) A simple ultraviolet spectrophotometric method for the determination of protein. *J. Lab. Clin. Med.* 48, 311-314.
22. Schagger, H., and von Jagow, G. (1987) Tricine-sodium dodecyl sulfate-polyacrylamide gel electrophoresis for the separation of proteins in the range of 1 to 100 kDa. *Anal. Biochem.* 166, 368-379.



- 1  
2  
3  
4  
5  
6  
7  
8  
9  
10  
11  
12  
13  
14  
15  
16  
17  
18  
19  
20  
21  
22  
23  
24  
25  
26  
27  
28  
29  
30  
31  
32  
33  
34  
35  
36  
37  
38  
39  
40  
41  
42  
43  
44  
45  
46  
47  
48  
49  
50  
51  
52  
53  
54  
55  
56  
57  
58  
59  
60
23. Laemmli, U. K. (1970) Cleavage of structural proteins during the assembly of the head of bacteriophage T4. *Nature* 227, 680-685.
24. Whitman, C.P., Aird, B.A., Gillespie, W.R., and Stolowich, N.J. (1991) Chemical and enzymatic ketonization of 2-hydroxymuconate, a conjugated enol. *J. Am. Chem. Soc.* 113, 3154-3162.
25. Johnson Jr., W.H., Hajipour, G., and Whitman, C.P. (1995) Stereochemical studies of 5-(carboxymethyl)-2-hydroxymuconate isomerase and 5-(carboxymethyl)-2-oxo-3-hexene-1,6-dioate decarboxylase from *Escherichia coli* C: mechanistic and evolutionary implications. *J. Am. Chem. Soc.* 117, 8719-8726.
26. Zimmermann, J., and Seebach, D. (1987) Brominations of cyclic acetals from  $\alpha$ -amino acids and  $\alpha$ - or  $\beta$ -hydroxy acids with N-bromosuccinimide. *Helv. Chim. Acta* 70, 1104-1114.
27. Burk, M.J., Feaster, J.E., and Harlow, R.L. (1991) New chiral phospholanes; synthesis, characterization, and use in asymmetric hydrogenation reactions. *Tetrahedron: Asymmetry* 2, 569-592.
28. Uchikawa, O., Okukado, N., Sakata, T., Arase, K., and Terada, K. (1988) Synthesis of (*S*)- and (*R*)-3-hydroxy-4-butanolide and (2*S*,4*S*)-, (2*R*,4*S*)-, (2*S*,4*R*)-, and (2*R*,4*R*)-2-hydroxy-4-hydroxymethyl-4-butanolide and their satiety and hunger modulating activities. *Bull. Chem. Soc. Jpn.* 61, 2025-2029.
29. Schroeder, G. K., Johnson, W. H., Jr., Huddleston, J. P., Serrano, H., Johnson, K. A., and Whitman, C. P. (2012) Reaction of *cis*-3-chloroacrylic acid dehalogenase with an allene substrate, 2,3-butadienoate: hydration via an enamine. *J. Am. Chem. Soc.* 134, 293-304.

- 1  
2  
3 30. Karplus, M. (1963) Vicinal proton coupling in nuclear magnetic resonance. *J. Am. Chem.*  
4 *Soc.* 85, 2870-2871.  
5  
6  
7  
8 31. Wu, J., Jiang, C., Wang, B., Ma, Y., Liu, Z., and Liu, S. (2006) Novel partial reductive  
9 pathway for 4-chloronitrobenzene and nitrobenzene degradation in *Comamonas* sp. strain  
10 CNB-1. *Appl. Environ. Microbiol.* 72, 1759-1765.  
11  
12  
13 32. Ma, Y-F., Wu, J-F., Wang, S-Y., Jiang, C-Y., Zhang, Y., Qi, S-W., Liu., L., Zhao, G-P.,  
14 and Liu, S-J. (2007) Nucleotide sequence of plasmid pCNB1 from *Comamonas* strain  
15 CNB-1 reveals novel genetic organization and evolution for 4-chloronitrobenzene  
16 degradation. *Appl. Environ. Microbiol.* 73, 4477-4483.  
17  
18  
19 33. Bhowmik, S., Horsman, G., Bolin, J.T., and Eltis, L.D. (2007) The molecular basis for  
20 inhibition of BphD, a C-C bond hydrolase involved in polychlorinated biphenyls  
21 degradation: large 3-substituents prevent tautomerization. *J. Biol. Chem.* 282, 36377-  
22 36385.  
23  
24  
25 34. Adams, L., and Ghiorse, W. C. (1985) Influence of manganese on growth of a sheathless  
26 strain of *Leptothrix discophora*. *Appl. Environ. Microbiol.* 49, 556-562.  
27  
28  
29  
30  
31  
32  
33  
34  
35  
36  
37  
38  
39  
40  
41  
42  
43  
44  
45  
46  
47  
48  
49  
50  
51  
52  
53  
54  
55  
56  
57  
58  
59  
60

**Table 1.** Summary of Specific Rotations  $[\alpha]^{20}_{\text{D}}$  and Stereochemical Assignments for **15**, **16**, and **17**<sup>a</sup>.

Product (substrate)	<i>P. putida</i>	<i>L. cholodnii</i>	Solvent	Assignment
<b>15 (10)</b>	+16°	+16°	methanol	<i>S</i> <sup>b</sup>
<b>16 (11)</b>	+40°	+38°	chloroform	<i>S</i> <sup>c</sup>
<b>17 (12)</b>	+87°	+88°	methanol	<i>R</i> <sup>d</sup>

<sup>a</sup>The rotations were measured in a 10 cm sample cell and standardized at 1 g/mL of the indicated solvent. <sup>b</sup>Reference 26. <sup>c</sup>Reference 27. <sup>d</sup>Reference 28.

## SCHEME LEGENDS

Scheme 1. The bacterial degradation of a monocyclic aromatic compound to pyruvate and acetyl CoA by the meta-fission pathway. The VPH-catalyzed conversion of **2** to (4*S*)-**4** via **3** is shown.

Scheme 2. The reaction catalyzed by the 4-OD/VPH complex in *P. putida* mt-2.

Scheme 3. The substrates and products for VPH used in this report.

Scheme 4. The series of enzyme-catalyzed reactions used to convert 5-substituted-2-hydroxymuconates to the 5-substituted-2-keto-4-hydroxypentanoates.

Scheme 5. The chemical degradation routes used to assign the stereochemistry at C-4 of **4**, **8**, and **9**.

Scheme 6. The stereochemical assignments for 3,5-[di-D]-**8** and **9** in the assumed conformation.

Scheme 7. Partial catabolic pathway for phenylpropionate (**18**) in *E. coli* C showing MhpD, the VPH isoform.

Scheme 8. Partial catabolic pathway for phenylalanine and tyrosine in *E. coli* C, showing the reaction catalyzed by HpcG.

Scheme 9. The proposed mechanism for OHED hydratase, showing the  $\alpha,\beta$ -unsaturated ketone (23).

Scheme 10. Different conformations for (3*S*,4*S*,5*S*)-21.

Scheme 11. The proposed 5-halo intermediates in a proposed haloaromatic catabolic pathway in *Comamonas* sp. strain CNB-1.

FIGURE LEGENDS

**Figure 1.** Partial <sup>1</sup>H NMR spectrum (600 MHz) of A) fully protio (4*S*)-**8**, (B) (3*S*,4*S*,5*S*)-3,5-[di-D]**8** generated by the 4-OD/VPH complex from *P. putida* mt-2, and (C) (3*S*,4*S*,5*S*)-3,5-[di-D]**8** generated by the 4-OD/VPH complex from *L. cholodnii*. The doublets with asterisks above them in B) and C) correspond to impurities, as described in the text. The DMSO is d<sub>6</sub>-labeled.

**Figure 2.** Partial <sup>1</sup>H NMR spectrum (600 MHz) of A) fully protio (4*R*)-**9**, (B) (3*S*,4*R*,5*R*)-3,5-[di-D]**9** generated by the 4-OD/VPH complex from *P. putida* mt-2, and (C) (3*S*,4*R*,5*R*)-3,5-[di-D]**9** generated by the 4-OD/VPH complex from *L. cholodnii*.

**Figure 3.** The proposed mechanism for OHED hydratase in D<sub>2</sub>O (adapted from Izumi et al.)<sup>12</sup>  
The roles of the implicated active site residues are shown and discussed in the text.

Figure 1.

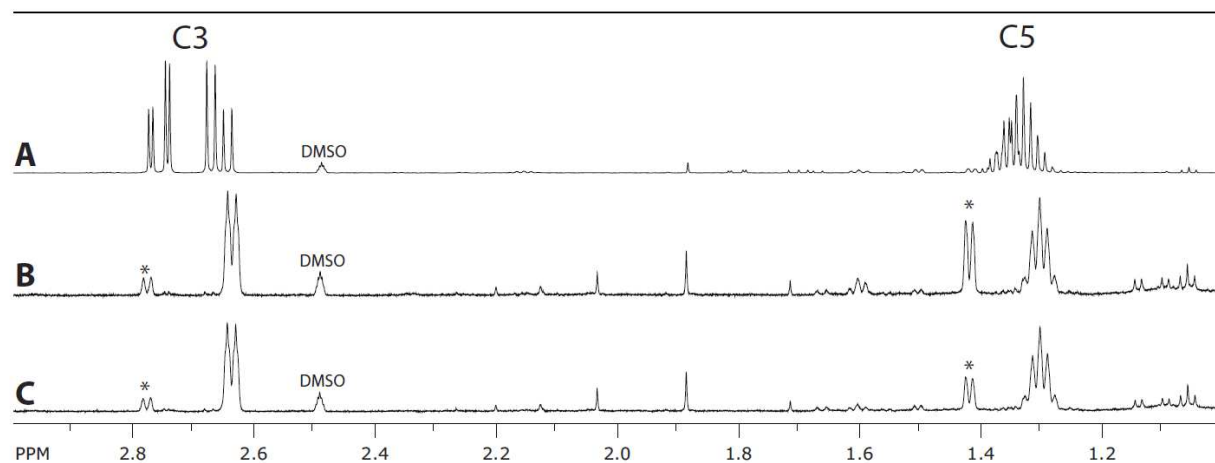
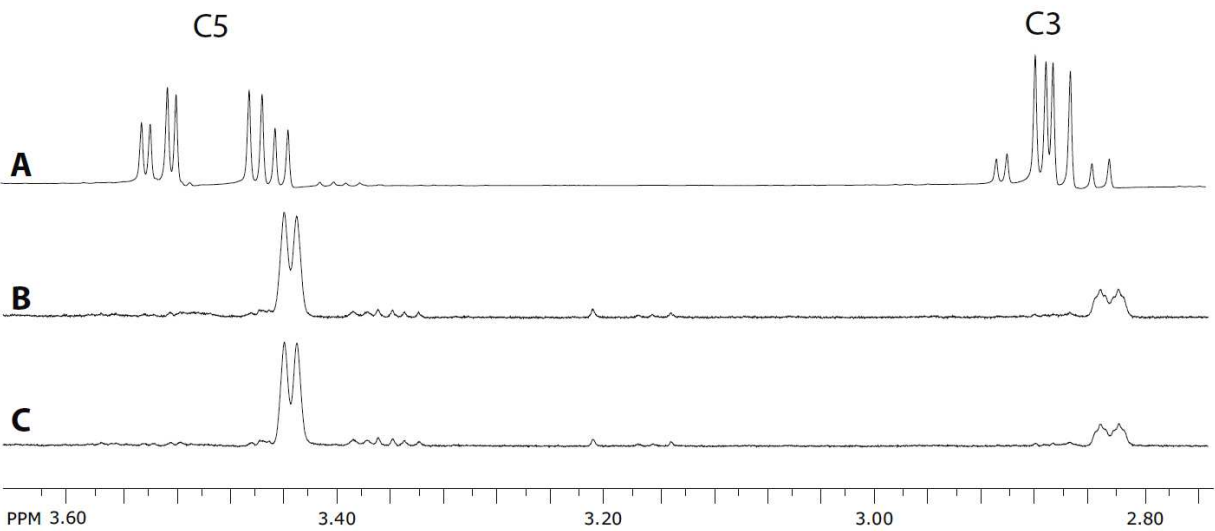


Figure 2.





**Figure 3.**

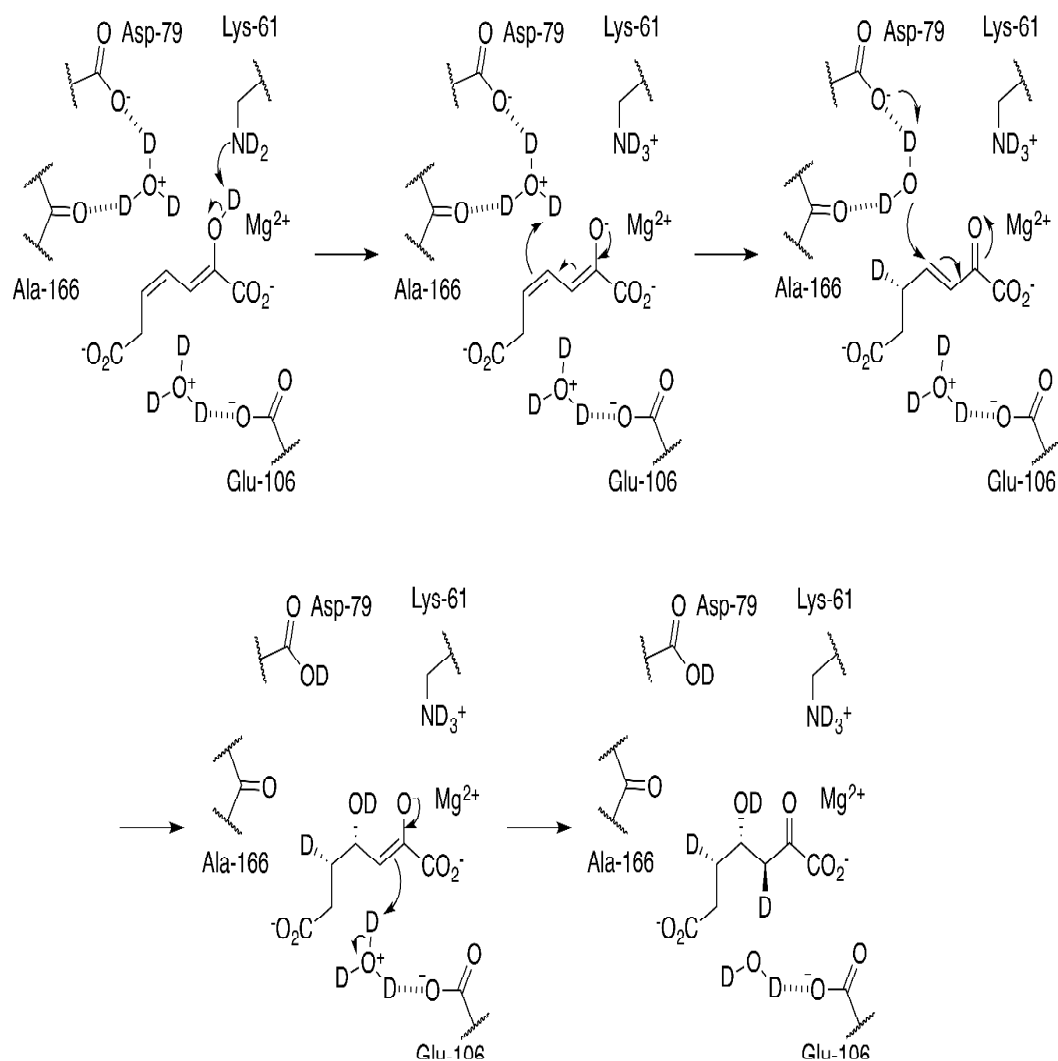
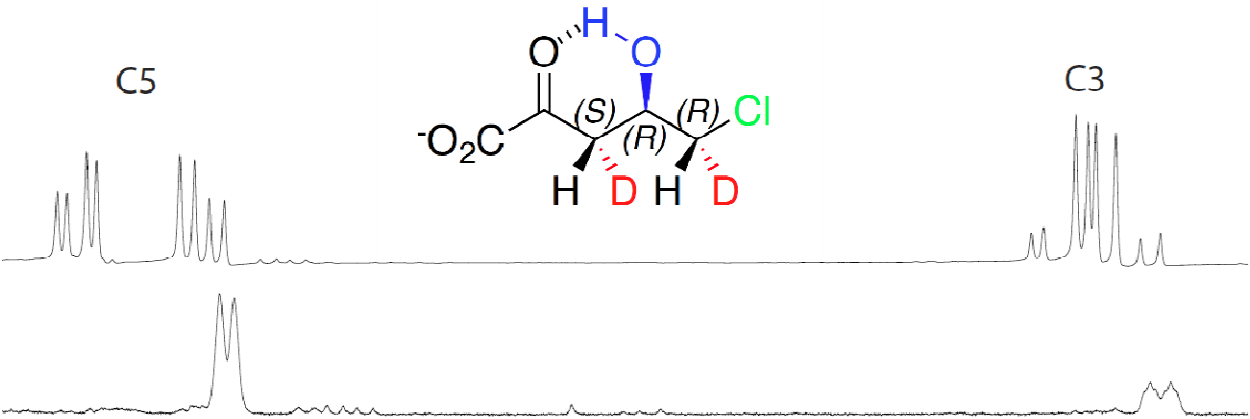


Table of Contents Graphic.



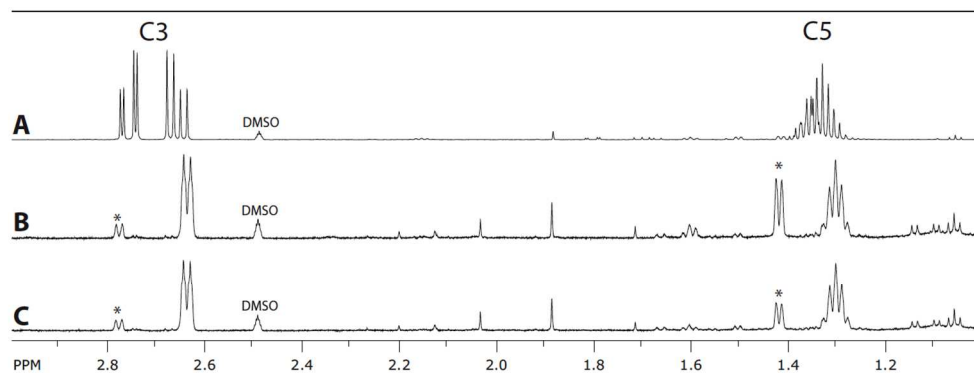


Figure 1

365x203mm (100 x 100 DPI)

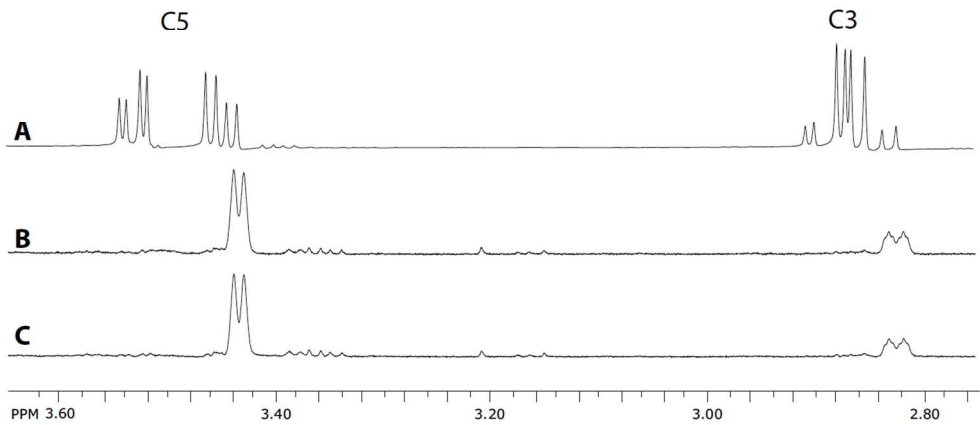


Figure 2

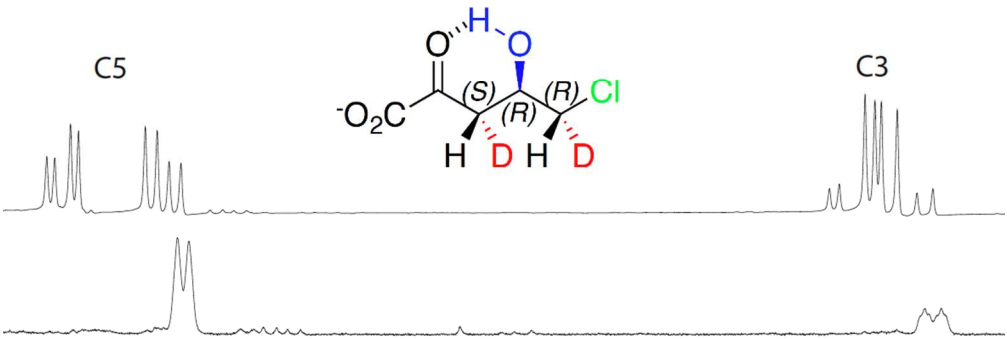
365x203mm (100 x 100 DPI)

## Unable to Convert Image

The dimensions of this image (in pixels) are too large to be converted. For this image to convert, the total number of pixels (height x width) must be less than 40,000,000 (40 megapixels).

Figure 3

1  
2  
3  
4  
5  
6  
7  
8  
9  
10  
11  
12  
13  
14  
15  
16  
17  
18  
19  
20  
21  
22  
23  
24  
25  
26  
27  
28  
29  
30  
31  
32  
33  
34  
35  
36  
37  
38  
39  
40  
41  
42  
43  
44  
45  
46  
47  
48  
49  
50  
51  
52  
53  
54  
55  
56  
57  
58  
59  
60



TOC

299x112mm (100 x 100 DPI)